Human-Data Based Cost of Bipedal Robotic Walking*

Aaron D. Ames
Mechanical Engineering
Texas A&M University
College Station, TX 77843
aames@tamu.edu

Ram Vasudevan
Electrical Engineering and Computer Sciences
University of California, Berkeley
Berkeley, CA 94720
ramv@eecs.berkeley.edu

Ruzena Bajcsy
Electrical Engineering and Computer Sciences
University of California, Berkeley
Berkeley, CA 94720
bajcsy@eecs.berkeley.edu

ABSTRACT

This paper proposes a cost function constructed from human data, the *human-based cost*, which is used to gauge the "human-like" nature of robotic walking. This cost function is constructed by utilizing motion capture data from a 9 subject straight line walking experiment. Employing a novel technique to process the data, we determine the times when the number of contact points change during the course of a step which automatically determines the ordering of discrete events or the *domain breakdown* along with the amount of time spent in each domain. The result is a weighted graph or *walking cycle*, associated with each of the subjects walking gaits. Finding a weighted cycle that minimizes the cut distance between this collection of graphs produces an *optimal* or *universal* domain graph for walking together with an *optimal walking cycle*. In essence, we find a single domain graph and the time spent in each domain that yields the most "natural" and "human-like" bipedal walking. The human-based cost is then defined as the cut distance from this optimal gait. The main findings of this paper are two-fold: (1) when the human-based cost is computed for subjects in the experiment it detects medical conditions that result in aberrations in their walking, and (2) when the human-based cost is computed for existing robotic models the more human-like walking gaits are correctly identified.

Categories and Subject Descriptors

I.6.8 [**Simulation and Modeling**]: Types of Simulation—*Continuous, Discrete Event*

General Terms

Theory

*This research is supported in part by NSF Awards CCR-0325274, CNS-0953823, ECCS-0931437, IIS-0703787, IIS-0724681, IIS-0840399 and NHARP Award 000512-0184-2009.

HSCC'11, April 12–14, 2011, Chicago, Illinois, USA.

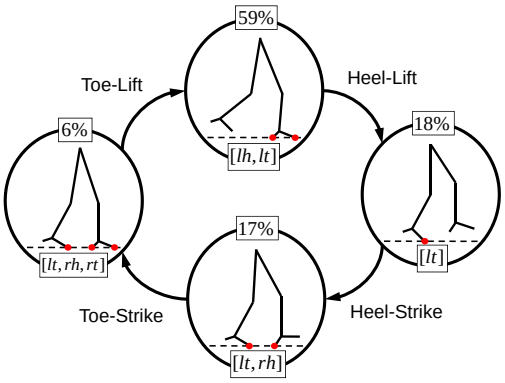

Figure 1: An example of a *domain breakdown*, i.e., the discrete phases of a walking gait, based upon a specific temporal ordering. The red dots indicate the constraints enforced in each discrete phase (or domain).

Keywords

Bipedal walking, Gait design, Human locomotion, Hybrid systems, Cost functions

1. INTRODUCTION

While constructing a bipedal walking robot, beyond the immediate goal of obtaining stable walking, a cost function is generally chosen to optimize certain system parameters. The choice of a cost function can have a dramatic impact on the resulting gait. In contrast to other robotic applications, the goal of bipedal walking is typically not to minimize the energy expended but rather to achieve the more nebulous goal of natural or human-like walking. The most popularly chosen cost function to obtain bipedal walking are torque squared [5, 11, 20] or the specific cost of transport [8, 12, 15]; however, no clear connection exists between minimizing these types of costs and achieving anthropomorphic walking. This lack of connection motivates the question: can a cost function be constructed that, when minimized, produces human-like gait?

This paper proposes a cost function based upon human-walking data: the *human-based cost*, built upon the idea of comparing the *temporal ordering of events* for humans and robots and, more specifically, the amount of time spent in each successive domain. One of the most important decisions made during the design of controllers for bipedal robots

is the temporal ordering of events that occur during the walking gait, i.e., the discrete phases (or *domains*) of the walking termed a *domain breakdown*. This decision alone determines the constraints that are enforced at any given time during the walking gait, and thus determines the continuous dynamics (through holonomic constraints) on each phase and the discrete dynamics (impact equations) between each phase. Therefore, given the equations of motion for a bipedal robot, the temporal ordering of events completely determines the mathematical model for the biped. The temporal ordering of events not only determines the underlying mathematical model of a bipedal robot, but is essential during control design; specific controllers are often designed or constrained by the specific choice of domain breakdown. When controllers are obtained that yield a walking gait, this gait is again related back to the domain breakdown since one can consider the amount of time spent in each discrete domain. The end result is a weighted cycle associated to a walking gait, termed a *walking cycle* (see Fig. 1 for an example).

Given the domain breakdown's significance, this paper proposes employing walking cycles collected from human walking experiments to develop a cost function, the human-based cost, that judges the "human-like" nature of a specific gait. We begin by considering a 9 subject straight line walking experiment recorded using motion capture. From this data, we develop a novel and automatic method for determining the domain breakdown of each subject. The end result is a collection of walking cycles. We then find the cycle graph and associated weighting that is the minimum cut distance between all of the subjects, termed the *optimal walking cycle*, which gives a "universal" domain breakdown and associated walking cycle for walking. The human-based cost is the cut distance between a walking cycle and the optimal walking cycle. To demonstrate the usefulness of the proposed cost function we compute the human-based cost for both the subjects in the experiment along with existing robotic models. When the human-based cost is computed for the subjects in the experiment we are able to automatically find preexisting medical conditions without *a priori* knowledge of such conditions. Computing the human-based cost for existing bipedal robotic models confirms that robotic gaits that are more anthropomorphic in nature have a lower human-based cost.

The applications of the results of this paper have the potential to be far-reaching in the bipedal robotic community. There is currently a fractured landscape when one considers only domain breakdowns. Most models assume a single domain model [9, 18, 20] which we show in this paper, even under the best case scenario, results in an unnatural gait due to their high human-based cost. When bipedal models are extended beyond a single domain, there is no unity as to which domain breakdown should be used; temporal orderings have been chosen ranging from one discrete phase to five, e.g., [10] considers one, [1, 6, 7, 13, 19] considers two, [16, 19] considers three, [4, 11] considers four, and [17] considers five. This lack of consistency among models in the literature motivates the desire to determine if there does in fact exist a single "universal" domain breakdown that should be used when modeling bipedal robots, especially in the context of obtaining human-like bipedal walking. This is what the optimal walking cycles that are determined in this paper offer.

It is important to note that human gait has been studied at great length by the biomechanics community [2, 21, 22, 23]. This work has focused almost entirely on either understanding the kinematic nature of human gait or muscle coordination during human gait. In contrast to these classical biomechanics approaches, we use human data to determine the temporal ordering of events. Since a temporal ordering of events is crucial in determining the dynamical model of a biped, the discovery of a "universal" temporal ordering could dramatically aide in the development of a bipedal robot with an anthropomorphic gait.

2. FROM CONSTRAINTS TO MODELS

Bipedal robots display both discrete and continuous behavior, i.e., they are naturally modeled as *hybrid systems*. Bipeds evolve in a continuous fashion according to traditional equations of motion when a fixed number of points on the biped are in contact with the ground, e.g., when one foot is flat on the ground while the other swings forward. The discrete behavior in the system occurs when the number of contact points changes.

In this section, we formally introduce hybrid systems and discuss how the equations of motion of a robot together with a temporal ordering of constraints completely determines the hybrid model of the system. That is, when modeling bipedal robots, one needs only the Lagrangian of the robot and a domain breakdown.

2.1 Hybrid Systems.

Hybrid systems (or *systems with impulse effects*) have been studied extensively in a wide variety of contexts and have been utilized to model a wide range of bipedal robotic models. In this section, we introduce a definition of a hybrid system applicable to bipedal walking.

Graphs and Cycles. A graph is a tuple $\Gamma = (V, E)$, where V is the set of vertices and $E \subset V \times V$ is the set of edges; an edge $e \in E$ can be written as $e = (i, j)$, and the source of e is $\text{source}(e) = i$ and the target of e is $\text{target}(e) = j$. Since steady state bipedal walking is naturally periodic, we are interested in hybrid systems *on a cycle*; therefore, we are interested in graphs that contain cycles or are themselves cycles. A *directed cycle* (or just a cycle) is a graph $\ell = (V, E)$ such that the edges and vertices can be written as:

$$\begin{aligned} V &= \{v_0, v_1, \ldots, v_{p-1}\}, \\ E &= \{e_0 = (v_0, v_1), \ldots, e_{p-1} = (v_{p-1}, v_0)\}. \end{aligned} \tag{1}$$

Since in the case of a cycle, the edges are completely determined by the vertices, we sometimes simply denote a cycle by: $\ell : v_0 \to v_1 \to \cdots \to v_{p-1}$. In the case when a graph Γ is being considered with more than one cycle, we denote a cycle in the graph by $\ell \subset \Gamma$.

Example 1. *The domain graph pictured in Fig. 1 has an underlying graph that is a directed cycle: $\Gamma_u = (V_u, E_u)$. In particular, there are 4 vertices and edges, which results in the cycle:*

$$\ell_u : [lh, lt] \to [lt] \to [lt, rh] \to [lt, rh, rt].$$

With the notion of a directed cycle, we can introduce the formulation of a hybrid system that is of interest in this paper.

Definition 1. *A* hybrid system in a cycle *is a tuple*

$$\mathscr{HC} = (\ell, D, U, S, \Delta, FG),$$

where

- $\ell = (V, E)$ *is a directed cycle*
- $D = \{D_v\}_{v \in V}$ *is a set of domains, where* $D_v \subseteq \mathbb{R}^{n_v} \times \mathbb{R}^{m_v}$ *is a smooth submanifold of* $\mathbb{R}^{n_v} \times \mathbb{R}^{m_v}$ *(with* $\mathbb{R}^{m_v}$ *representing control inputs),*
- $U = \{U_v\}_{v \in V}$*, where* $U_v \subset \mathbb{R}^{m_v}$ *is a set of admissible controls,*
- $S = \{S_e\}_{e \in E}$ *is a set of guards, where* $S_e \subseteq D_{\text{source}(e)}$*,*
- $\Delta = \{\Delta_e\}_{e \in E}$ *is a set of reset maps, where* $\Delta_e : \mathbb{R}^{n_{\text{source}(e)}} \to \mathbb{R}^{n_{\text{target}(e)}}$ *is a smooth map,*
- $FG = \{(f_v, g_v)\}_{v \in E}$*, where* (f_v, g_v) *is a control system on* D_v*, i.e.,* $\dot{x} = f_v(x) + g_v(x)u$ *for* $x \in D_v$ *and* $u \in U_v$*.*

2.2 Hybrid Systems from Constraints.

The remainder of this section illustrates how a Lagrangian for the biped, together with a domain breakdown (which determines the active constraints on each vertex of a directed cycle), allows one to explicitly construct a hybrid model of the system. Many details of this construction summarize the procedure presented in [11].

2.2.1 General Setup

We begin with a bipedal robot either in two or three dimensions—the discussion in this paper is applicable to either case. We first construct a Lagrangian for the biped when no assumptions on ground contact are made and then enforce the ground contact conditions through constraints as determined by the domain graph.

Lagrangians. Let R_0 be a fixed inertial or world frame, and R_b be a reference frame attached to the body of the biped with position $p_b \in \mathbb{R}^3$ and orientation $\phi_b \in SO(3)$. Consider a configuration space for the biped Q_r, i.e., a choice of (body or shape) coordinates for the robot where typically $q_r \in Q_r$ is a collection of (relative) angles between each successive link of the robot. The *generalized* coordinates of the robot are then given by $q = (p_b^T, \phi_b^T, q_r)^T \in Q = \mathbb{R}^3 \times SO(3) \times Q_r$, with Q the generalized configuration space.

The Lagrangian of a bipedal robot, $L : TQ \to \mathbb{R}$, can be stated in terms of kinetic and potential energies as:

$$L(q, \dot{q}) = K(q, \dot{q}) - V(q).$$

The Euler-Lagrange equations yield the equations of motion, which for robotic systems [14] are stated as:

$$D(q)\ddot{q} + H(q, \dot{q}) = B(q)u, \tag{2}$$

where $D(q)$ is the inertia matrix, $B(q)$ is the torque distribution matrix (and only depends on q_r), $B(q)u$ is the vector of actuator torques and $H(q, \dot{q}) = C(q, \dot{q})\dot{q} + G(q) - \Gamma(q, \dot{q})$ contains the Coriolis, gravity terms and non-conservative forces grouped into a single vector.

Contact Points. The continuous dynamics of the system depend on which constraints are enforced at any given time, while the discrete dynamics depend only on the temporal ordering of constraints. Constraints and their enforcement are dictated by the number of contact points of the system with the ground. Specifically, the *set of contact points* is the set $\mathcal{C} = \{c_1, c_2, \ldots, c_k\}$, where each c_i is a specific type of contact possible in the biped, either with the ground or in the biped itself (such as the knee locking).

If the knees do not lock, and assuming reasonable behavior by the feet, e.g., no standing on one corner of the foot, there are four contact points of interest given by:

$$\mathcal{C}_u = \{lh, lt, rh, rt\},$$

where lh and lt indicate the left heel and toe, and rh and rt indicate right heel and toe, respectively. If the knees lock, additional contact points for the left and right knee, lk and rk, must be considered. This yields a set of contact points:

$$\mathcal{C}_l = \{lh, lt, lk, rh, rt, rk\}.$$

Constraints. Contact points introduce a *holonomic constraint* on the system, η_c for $c \in \mathcal{C}$, which is a vector valued function $\eta_c : Q \to \mathbb{R}^{n_c}$, that must be held constant for the contact point to be maintained, i.e., $\eta_c(q) = \text{constant} \in \mathbb{R}^{n_c}$ fixes the contact point but allows rotation about this point if feasible. It is useful to express the collection of all holonomic constraints in a single matrix $\eta(q) \in \mathbb{R}^{n_c \times |\mathcal{C}|}$ as:

$$\eta(q) = \begin{bmatrix} \eta_{lh}(q) & 0 & 0 & 0 \\ 0 & \eta_{lt}(q) & 0 & 0 \\ 0 & 0 & \eta_{rh}(q) & 0 \\ 0 & 0 & 0 & \eta_{rt}(q) \end{bmatrix}$$

where $n = \sum_{c \in \mathcal{C}} n_c$. To determine the holonomic constraints for the contact points of interest, i.e., $\mathcal{C}_u$ and $\mathcal{C}_l$, two cases must be considered: one for foot contact points and another for knee contact.

In the case of foot contact, consider a reference frame R_c at the contact point $c \in \{lh, lt, rh, rt\}$ such that the axis of rotation about this point (either the heel or toe) is in the z direction. Then the rotation matrix between R_0 and R_c can be written as the product of three rotation matrices $Rot(x, \phi_c^z)Rot(y, \phi_c^y)Rot(z, \phi_c^z)$ and the position and orientation of R_c relative to R_0 is given as $\eta_c(q) = (p_c(q)^T, \phi_c^x, \phi_c^y)^T$, where $p_c(q)$ is the position of c, since ϕ_c^z is free to move while ϕ_c^x and ϕ_c^y must be held constant. The end result of this choice of coordinates is a holonomic constraint $\eta_c(q) = \text{constant}$, which fixes the foot contact point to the ground but allows rotation about the heel or toe depending on the specific type of foot contact. In the case of knee contact, let q_c, $c \in \{lk, rk\}$, be the relative angle of the left or right knee. The holonomic constraint is then given by $\eta_c(q) = q_c$, and enforcing the constraint $\eta_c(q) = 0$ keeps the knee locked.

Another class of constraints that are important are *unilateral constraints*, h_c for $c \in \mathcal{C}$, which are scalar valued functions, $h_c : Q \to \mathbb{R}$, that dictate the set of admissible configurations of the system; that is $h_c(q) \geq 0$ implies that the configuration of the system is admissible for the contact point c. Again, there are two types of these constraints to consider depending on whether foot or knee contact is being considered. In the case of foot contact, assuming that the walking is on flat ground, these constraints require the height of a contact point above the ground be non-negative: $h_c(q) = p_c^y(q) \geq 0$. In the case of knee contact, these constraints require the angle of the knee be positive: $h_c(q) = q_c \geq 0$. These constraints can be put in the form of a matrix $h(q) \in \mathbb{R}^{|Q| \times |Q|}$ in the same manner as the holonomic constraints.

Domain Breakdowns. A domain breakdown is a directed cycle together with a specific choice of contact points on every vertex of that graph. To define this formally, we assign to each vertex a binary vector describing which contact points are active in that domain.

Definition 2. *Let $\mathcal{C} = \{c_1, c_2, \ldots, c_k\}$ be a set of contact points and $\ell = (V, E)$ be a cycle. A domain breakdown is a function $\mathcal{B} : \ell \to \mathbb{Z}_2^k$ such that $B(v)_i = 1$ if c_i is in contact on v and $B(v)_i = 0$ otherwise.*

Example 2. *In the case of the graph Γ_u given in Example 1 and set of contact points $\mathcal{C} = \{lh, lt, rh, rt\}$, for the domain breakdown given in Fig. 1, this domain breakdown is formally given by $\mathcal{B}_u : \ell_u \to \mathbb{Z}_2^4$ where $\mathcal{B}_u([lh, lt])$, $\mathcal{B}_u([lt])$, $\mathcal{B}_u([lt, rh])$ and $\mathcal{B}_u([lt, rh, rt])$ are given by:*

$$\mathcal{B}_u(\ell): \begin{bmatrix} 1 \\ 1 \\ 0 \\ 0 \end{bmatrix} \to \begin{bmatrix} 0 \\ 1 \\ 0 \\ 0 \end{bmatrix} \to \begin{bmatrix} 0 \\ 1 \\ 1 \\ 0 \end{bmatrix} \to \begin{bmatrix} 0 \\ 1 \\ 1 \\ 1 \end{bmatrix}.$$

2.2.2 Hybrid System Construction

We now demonstrate that given a Lagrangian, a directed cycle, and a domain breakdown, a hybrid system can be explicitly constructed. Since the Lagrangian is intrinsic to a robot, this result proves that a domain breakdown, which is determined by the enforced contact points, alone dictates the mathematical model of a biped.

Continuous Dynamics. We explicitly construct the control system $\dot{x} = f_v(x) + g_v(x)u$ through the constraints imposed on each domain through the domain breakdown.

For the domain $v \in V$, the holonomic constraints that are imposed on that domain are given by:

$$\eta_v(q) = \eta(q)\mathcal{B}(v),$$

where the domain breakdown dictates which constraints are enforced. Differentiating the holonomic constraint yields a *kinematic constraint*:

$$J_v(q)\dot{q} = 0,$$

where $J_v(q) = \text{RowBasis}\left(\frac{\partial \eta_v(q)}{\partial q}\right)$ is a basis for the row space of the Jacobian (this removes any redundant constraints so that J_v has full row rank). The kinematic constraint yields the *constrained dynamics* on the domain:

$$D(q)\ddot{q} + H(q, \dot{q}) = B(q)u + J_v(q)^T F_v \tag{3}$$

which enforces the holonomic constraint; here D, H and B are as in Equation (2) and F_v is the *wrench* containing forces and moments expressed in the reference frame R_c [14]. To determine the wrench F_v, we differentiate the kinematic constraint:

$$J_v(q)\ddot{q} + \frac{\partial J_v(q)}{\partial q}\dot{q} = 0$$

and combine this equation with Equation (3) to obtain an expression for $F_v(q, \dot{q}, u)$ which is affine in u. Therefore, for $x = (q^T, \dot{q}^T)^T$, Equation (3) yields the affine control system $\dot{x} = f_v(x) + g_v(x)u$.

Discrete Dynamics. We now construct the domains, guards and reset maps for a hybrid system using the domain breakdown.

Given a vertex $v \in V$, the domain is the set of admissible configurations of the system factoring in both friction and a unilateral constraint. Specifically, from the wrench $F_v(q, \dot{q}, u)$, one can ensure that the foot does not slip by considering inequalities on the friction which can be stated in the form: $\mu_v(q)^T F_v(q, \dot{q}, u) \geq 0$, with $\mu_v(q)$ a matrix of friction parameters and constants defining the geometry of the foot (see [11] for more details). These are coupled with the unilateral constraint on this domain, $h_v(q) = h(q)\mathcal{B}(v)$, to yield the set of admissible configurations:

$$A_v(q, \dot{q}, u) = \begin{bmatrix} \mu_v(q)^T F_v(q, \dot{q}, u) \\ h_v(q) \end{bmatrix} \geq 0. \tag{4}$$

The domain is thus given by:

$$D_v = \{(q, \dot{q}, u) \in TQ \times \mathbb{R}^{m_v} : A_v(q, \dot{q}, u) \geq 0\}.$$

The guard is just the boundary of this domain with the additional assumption that set of admissible configurations is decreasing, i.e., the vector field is pointed outside of the domain, or for an edge $e = (v, v') \in E$,

$$G_e = \{(q, \dot{q}, u) \in TQ \times \mathbb{R}^{m_v} : A_v(q, \dot{q}, u) = 0 \text{ and } \dot{A}_v(q, \dot{q}, u) \leq 0\}.$$

The impact equations are given by considering the constraints enforced on the subsequent domain. For an edge $e = (q, q') \in E$, the post-impact velocity $\dot{q}^+$ is given in terms of the pre-impact velocity $\dot{q}^-$ by:

$$\dot{q}^+ = P_e(q, \dot{q}^-) = (I - D^{-1}J_{q'}^T(J_{q'}D^{-1}J_{q'}^T)^{-1}J_{q'})\dot{q}^-$$

with I the identity matrix. This yields the reset map[1]:

$$R_e(q, \dot{q}) = \begin{bmatrix} q \\ P_e(q, \dot{q}) \end{bmatrix}$$

The end result is that given a domain breakdown and a bipedal robot, the hybrid model for the biped is completely determined.

3. DOMAIN BREAKDOWNS FROM HUMAN DATA

In this section, we determine the domain breakdown for 9 human subjects during walking. We begin by discussing the experiment and how the data was handled. We then present a method for extracting the times when the constraint for a given contact point is enforced through a method that fits the "simplest" function to the motion of the contact point when it is not enforced; the time intervals during a step when the constraints are enforced are simply the times when this function is not being followed. The end result of this procedure is a temporal ordering of events, which yields a domain breakdown. The domain breakdowns for all 9 subjects are presented in the case of no knee-lock and knee-lock (the motivation for considering both cases is discussed further in this section).

Walking Experiment. Data was collected on 9 subjects using the Phase Space System[2], which computes the 3D position of 19 LED sensors at 480 frames per second using 12 cameras at 1 millimeter level of accuracy. The cameras

[1]Note that in order to get periodic behavior in the walking, the "left" and "right" leg must be "swapped" at one of the transitions; this "trick" is common throughout the literature.

[2]`http://www.phasespace.com/`

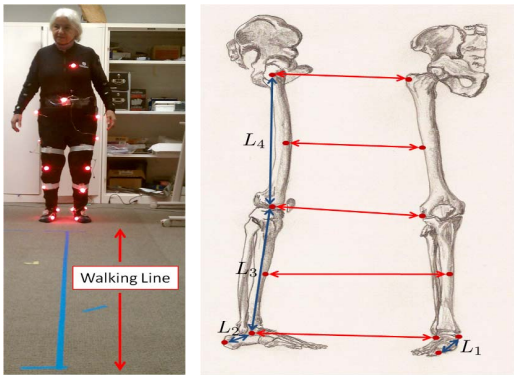

Figure 2: Illustrations of the experimental setup (left) and sensor placement on each foot (middle and right). Each LED sensor was placed at the joints as illustrated with the red dots on the right lateral (middle) and anterior aspects (right) of the each leg.

were calibrated prior to the experiment and were placed to achieve a 1 millimeter level of accuracy for a space of size 5 by 5 by 5 meters cubed. 8 LED sensors were placed on each leg at the joints on on the heel and toe, 1 LED sensor was placed on the sternum, 1 LED sensor was placed on the back behind the sternum, and 1 LED sensor was placed on the belly button. Each trial of the experiment required the subject to walk 3 meters along a line drawn on the floor. Each subject performed 12 trials, which constituted a single experiment. 3 female and 6 male subjects with ages ranging between 17 and 77, heights ranging between 161 and 189 centimeters, and weights ranging between 47.6 and 90.7 kilograms. Table 3 describes the measurements of each of the subjects. The data for each individual is then rotated so that the walking occurs in the x-direction and for each subject, the 12 walking trials are averaged (after appropriately shifting the data in time) which results in a single trajectory for each constraint for each subject for at least two steps (one step per leg); the resulting data can be seen in Fig. 4. Any interested researcher can perform analysis on the collected data[3].

[3] `http://www.eecs.berkeley.edu/~ramv/HybridWalker`

	Sex	Age	Weight	Height	L_1	L_2	L_3	L_4
1	M	30	90.7	184	14.5	8.50	43.0	44.0
2	F	19	53.5	164	15.0	8.00	41.0	44.0
3	M	17	83.9	189	16.5	8.00	45.5	55.5
4	M	22	90.7	170	14.5	9.00	43.0	39.0
5	M	30	68.9	170	15.0	8.00	43.0	43.0
6	M	29	59.8	161	14.0	8.50	37.0	40.0
7	M	26	58.9	164	14.0	9.00	39.0	41.0
8	F	77	63.5	163	14.0	8.00	40.0	42.0
9	F	23	47.6	165	15.0	8.00	45.0	43.0

Figure 3: Table describing each of the subjects. The subject number is in the left column and the L_1, L_2, L_3, L_4 measurements correspond to the lengths described in Fig. 2. The measurement in column 4 is in kilograms (and was self reported) and the measurements in columns 5-9 are in centimeters.

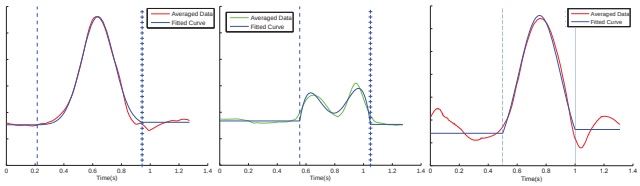

Figure 4: The data for the height of the heel (left), height of the toe (middle) and angle of the knee (right) together with the fittings of a constant, Gaussian, and constant for the heel (left), a constant, 4^{th} order polynomial, and constant for the toe (middle) and a constant, Gaussian, and constant for the knee (right). The vertical lines indicate the transitions points between the fitting functions.

Function Fitting. In order to determine the domain breakdowns for the subjects in the walking experiment, it is necessary to determine the times when the number of contact points change, i.e., the *event times*. Rather than looking for when the contact point is constrained (via thresholding), we choose a "simple" function that the contact point follows when unconstrained. When this function is not being followed, the constraints are enforced and thus constant. Therefore, once this function has been identified, the rest of the process to determine the domain breakdown becomes automatic.

To formalize the idea of function fitting to determine event times, given a set of contact points, $\mathcal{C}$, let $s_c(n, a)$ be the "simplest" function that the contact point $c \in \mathcal{C}$ follows while unconstrained ($a \in R^k$ is a vector that parameterizes the function). Denote the contact point sensor data by $y_c(n)$ where $n \in \{1, \ldots, T\}$. When the contact point is constrained the sensor data appears constant, and when the contact point is unconstrained the sensor data follows $s_c(n, a)$. We therefore define the function:

$$f_c(n, \tau_l, \tau_s, a) = \begin{cases} s_c(\tau_l, a) & \text{if} \quad n \leq \tau_l \\ s_c(n, a) & \text{if} \quad \tau_l < t_n < \tau_s \\ s_c(\tau_s, a) & \text{if} \quad \tau_s \leq n \end{cases}$$

where $\tau_l, \tau_s \in \{1, \ldots, T\}$ are the event times indicating when the contact point becomes unconstrained, τ_l (lift), and constrained, τ_s(strike)[4]. To determine the event times that best fit the data, we solve the following optimization problem:

$$\min_{\tau_l, \tau_s \in \{1, \ldots, T\}} \min_{a \in \mathbb{R}^k} \frac{1}{T} \sum_{n=1}^{T} |f_c(n, \tau_l, \tau_s, a) - y_c(n)|.$$

To illustrate this procedure, consider the averaged data plotted against time for the heel and toe contact point sensors in Fig. 4. Looking at this data, the behavior of the heel appears to follow a constant, followed by a Gaussian, followed by a constant; therefore, we claim that the "simplest" function that the heel follows when unconstrained is a Gaussian. In a similar fashion, the averaged data for the toe appears to follow a constant, followed by a 4^{th} order polynomial, followed by a constant. Using these observations, we fit the averaged heel and toe data to these functions using the described procedure. The results of this fitting are drawn in the same figure with the transition points τ_l and τ_s

[4] Here we assume without loss of generality that $\tau_l < \tau_s$.

indicated by vertical lines. The correlation coefficients for the illustrated heel and toe examples are 0.9968 and 0.9699, respectively.

Inspecting the data for the angle of the knee over time given in Fig. 4, one concludes that a human does not lock their knee through the course of walking, i.e., there is no period in which the knee is constant. In fact, there is clearly a period when the knee swings (the larger "bump") and a period when the knee goes through smaller oscillations. The smaller oscillations correspond to the period when the human has their weight on the knee, and the oscillations can be understood to be the natural spring and damping response of the muscles and tendons. Robotic bipedal walkers include a knee-lock domain since in practice it reduces energy consumption. Since we want to quantify how human-like such robotic walkers are, we do not want to disqualify the existence of knee-lock in the human data. It is for this reason that we consider both the case of knee-lock and no knee-lock.

One can view the period of smaller oscillations as the knee being "locked." Under this assumption, the "simplest" function that the knee follows is a constant, followed by a Gaussian, followed by a constant. The results of this fitting are drawn in Fig. 4 with the transition points τ_l and τ_s indicated by vertical lines.

Determining the Domain Breakdown. Given the data for a contact point $c \in \mathcal{C} = \{c_1, c_2, \ldots, c_k\}$, we determine the lift and strike times for the contact point, τ_l^c and τ_s^c, over the time interval of the averaged data using the aforementioned techniques. Since the data is over at least two steps (one step with each leg), there may be multiple lift and strike times over the period of the data. Using the aforementioned method we make no assumptions about simultaneous contact point enforcement. Denote by J_c the period where constraints associated with a contact point are enforced, i.e., $n \in J_c$ if $f_c(n) =$ constant with f_c the fitting function for the contact point $c \in \mathcal{C}$; these intervals are shown in blue in Fig. 5 over the course of one step (not the entire data period) in the case of $\mathcal{C}_u$ (or no knee-lock). Analogous to the definition of a domain breakdown (Def. 2), we can define a binary vector, $b(n) \in \mathbb{Z}_2^{|\mathcal{C}|}$, encoding which contact points are in force at any given time by letting $b(n)_i = 1$ if $n \in J_{c_i}$ and $b(n)_i = 0$ otherwise. This function only changes value a finite number of times and denotes these distinct values by $b(m), m = 0, 1 \ldots, M$.

To determine the domain breakdown associated with the walking, we begin by defining the directed cycle Γ (if it exists, which we do not assume). Looking at the data, we check to see if there exists an integer $p \in \mathbb{N}$ such that

$$b(m) = \begin{bmatrix} 0 & I \\ I & 0 \end{bmatrix} b(m+p)$$

for $0 \leq m \leq p$ with I the identity matrix and $0, I \in \mathbb{R}^{\frac{|\mathcal{C}|}{2} \times \frac{|\mathcal{C}|}{2}}$; the matrix that is multiplied by b serves the purpose of reordering the right and left leg. If this p can be found, periodic walking over the course of two steps exists with the left leg mirroring the behavior of the right leg. In this case, one constructs a directed cycle with p domains (as in Equation (1)) and this is the graph Γ. Finally, the domain breakdown $\mathcal{B}$ is given by $\mathcal{B}(v_m) = b(m)$. The application of this procedure to a single subject in the case of no knee-lock is illustrated in Fig. 5.

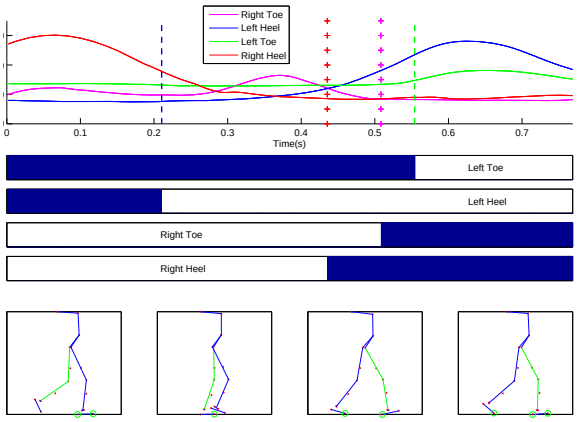

Figure 5: An overview of how the domain breakdown is achieved (with no knee-lock). The top row illustrates the height of the toe and heel of each leg over one step along with the lifting and strike time for each constraint (illustrated by vertical lines). The middle row illustrates which constraints are active based upon the fitting. The bottom row shows the resulting domain breakdown where enforced constraints are drawn with green circles.

Results. We perform the process outlined in this section on the set of contact points $\mathcal{C}_u = \{lh, lt, rh, rt\}$ and $\mathcal{C}_l = \{lh, lt, lk, rh, rt, rk\}$ on the 9 subjects that performed the walking experiment. The end result is that we find domain breakdowns for each subject, i.e., each subject had periodic walking. The domain breakdowns, along with the percentage of time spent in each domain in the case of no knee-lock and knee-lock for each individual, are illustrated in Fig. 6 and 8, respectively.

When knee-lock is not considered in the domain breakdown, observe that all subjects exhibit a *universal* domain breakdown shown in Fig. 1 in spite of great differences in age, height and weight. This is particularly surprising since we made no *a priori* assumptions about the ordering of contact point enforcement and did not demand simultaneous contact point enforcement. If we include knee-lock during the determination of the domain breakdown, there is not a single domain breakdown that is common to all subjects: out of the 9 subjects, there are 7 different domain breakdowns. This is probably due to the fact that humans do not actually lock their knees during walking. Nevertheless, during the design of a bipedal robot knee-lock can be an important domain to include since it can simplify the mechanical and controller development. In this instance, it is still useful to have a "universal" domain breakdown for the purposes of robotic design, and we construct such a "universal" domain breakdown in the next section by defining a distance metric on the space of domain breakdowns.

4. HUMAN-BASED COST OF WALKING

In this section, we construct a cost function that measures the anthropomorphic nature of robotic bipedal walking termed the *human-based cost*. We do this by first defining a metric on the space of weighted cycles, the *cut distance*, which allows us to compare different walking gaits and to construct an optimal walking cycle by minimizing the dis-

tance between the weighted cycles observed in the human walking data. Using the cut distance, we next define the *human-based cost* which allows us to compute the distance from a specific walking gait (either human or robotic) to the optimal walking cycle. The remainder of this section is devoted to using the human-based cost to determine the extent to which popular robotic models from the literature are anthropomorphic.

Distance Between Cycles. We employ the notion of *cut* (or *rectangular*) distance between two weighted graphs to compare different domain breakdowns (the definition in its general form can be found in [3]). Since we are only interested in the specific domains visited and the corresponding time spent in each of these domains, we define a notion of weighted cycle and a corresponding distance between weighted cycles that is pertinent to the application being considered.

Definition 3. *A walking cycle is a pair* (α, ℓ) *where* $\ell = (V, E)$ *is a cycle and* $\alpha : \ell \to \mathbb{R}^{|V|}$ *is a function such that* $\alpha(v) \geq 0$ *and* $\sum_{v \in V} \alpha(v) = 1$. *Denoting a cycle by* $\ell : v_0 \to v_1 \to \cdots \to v_p$, *we denote a walking cycle by:*

$$\alpha(\ell) : \alpha(v_0) \to \alpha(v_1) \to \cdots \to \alpha(v_p).$$

Example 3. *Each of the domain breakdowns presented in Fig. 6 gives us a distinct walking cycle. For example, Subject 1 has a walking cycle* $S_1 = (\alpha_1, \ell_1)$ *given by:*

$$\begin{array}{rcccccccc} \ell_1 & : & [lh, lt] & \to & [lt] & \to & [lt, rh] & \to & [lt, rh, rt] \\ \alpha_1(\ell_1) & : & 26.5\% & \to & 49.7\% & \to & 21.4\% & \to & 2.4\%. \end{array}$$

Here, and throughout this paper, weightings are stated in percentages to indicate the percentage of time the human spends in a domain through the course of one step.

We now introduce a definition of cut distance that is a slight modification of the definition presented in [3]. The only differences are that we do not force the weighted graphs to have nodes with positive weights, and we require the weights to sum to one.

Definition 4. *Let* (α_1, ℓ_1) *and* (α_2, ℓ_2) *be two walking cycles. Viewing both* α_1 *and* α_2 *as functions on* $V_1 \cup V_2$ *by letting* $\alpha_1(i) \equiv 0$ *if* $i \in V_2 \backslash V_1$ *and* $\alpha_2(j) \equiv 0$ *if* $j \in V_1 \backslash V_2$, *the cut distance between two cycles is given by:*

$$d(\alpha_1, \ell_1, \alpha_2, \ell_2) = \max_{I, J \subset V_1 \cup V_2} \left| \sum_{i \in I, j \in J} (\alpha_1(i)\alpha_1(j)\beta_1(i,j) - \alpha_2(i)\alpha_2(j)\beta_2(i,j)) \right| + \sum_{k \in V_1 \cup V_2} |\alpha_1(k) - \alpha_2(k)|, \quad (5)$$

where $\beta_1(i,j) = 1$ *for all edges* $(i,j) \in E_1$ *and* $\beta_2(i,j) = 1$ *for all edges* $(i,j) \in E_2$.

It is straightforward to check that the modified definition of the cut distance satisfies the requirements of a metric (i.e., non-negativity, identity of indiscernibles, symmetry and the triangle inequality). Intuitively, the cut distance compares just how different two walking cycles are when considering all possible "cuts" between the pair of cycles.

Human-Based Cost. The idea for developing a human-based cost of walking is that human walking data can be used to develop a cost function in which to judge other non-human walking. In the context of this paper, we develop a cost based upon the domain breakdown and resulting walking cycles associated with a subjects walking gait.

Definition 5. *Consider* N *subjects with associated domain breakdowns and walking cycles* $S_i = (\alpha_i, \ell_i)$ *for* $i \in \{1, \ldots, N\}$. *Letting* $\mathscr{L} = \bigcup_{i=1}^{N} \ell_i$ *be the graph obtained by combining all of the cycles* ℓ_i, *we define the optimal walking cycle by:*

$$(\alpha^*, \ell^*) = \operatorname*{argmin}_{(\alpha, \ell) \in \mathbb{R}^{|\ell|} \times \mathscr{L}} \frac{1}{N} \sum_{i=1}^{N} d(\alpha, \ell, \alpha_i, \ell_i). \quad (6)$$

The optimal walking cycle is just the walking cycle through the graph of all cycles obtained from the walking that best fits the data under the cut distance. The optimal walking cycle allows one to describe the extent to which a walking gait is human-like.

Definition 6. *Given a biped (either human or bipedal robot) with associated domain breakdown and walking cycle* $R = (\alpha_r, \ell_r)$, *the human-based cost (HBC) of walking is defined to be:*

$$\mathcal{H}(R) = d(\alpha_r, \ell_r, \alpha^*, \ell^*).$$

It is important to note that the optimal walking cycle may not be unique, and so there may be multiple HBCs of walking constructed from a single experiment, i.e., the HBC is not necessarily unique (in this paper, we found a unique HBC for the case of knee-lock, but multiple HBCs for the case of no knee-lock.) Unsurprisingly, multiple experiments might yield different optimal walking cycles and different HBCs, but if the experiments are carried out consistently they should be compatible and could be merged into a single HBC.

4.1 HBC without Knee-Lock

Using the walking cycles constructed from the human data illustrated in Fig. 6, we now compute the optimal walking cycle and compute the HBCs for the subjects and bipedal robots that have appeared in the literature. All subjects have the same universal cycle ℓ_u, so $S_i = (\alpha_i, \ell_u)$ for $i = 1, \ldots, 9$. The optimal walking cycle is given by (α^*, ℓ_u), where α^* is computed using Equation (6) yielding:

$$\begin{array}{rcccccccc} \ell_u & : & [lh, lt] & \to & [lt] & \to & [lt, rh] & \to & [lt, rh, rt] \\ \alpha^*(\ell_u) & : & 59\% & \to & 18\% & \to & 17\% & \to & 6\%. \end{array}$$

If the objective of a robotic biped is to obtain anthropomorphic walking, this optimal walking cycle should be followed as closely as possible. To demonstrate this, we use the optimal walking cycle to compute the HBC in several cases.

Humans. Although all of the subjects have a universal domain breakdown, this does not imply that they have identical walking gaits. To quantify the differences in walking between the different subjects, we compute the HBC for each subject. The results of this computation are illustrated in Fig. 7; for this comparison, the optimal walking cycle is computed using the data from all of the subjects and then each subject is compared to the optimal walking cycle, α^*, via the HBC. From these computations, it is clear that Subject 1 has an unusually high cost when compared to the other subjects whose costs are fairly uniform. In fact,

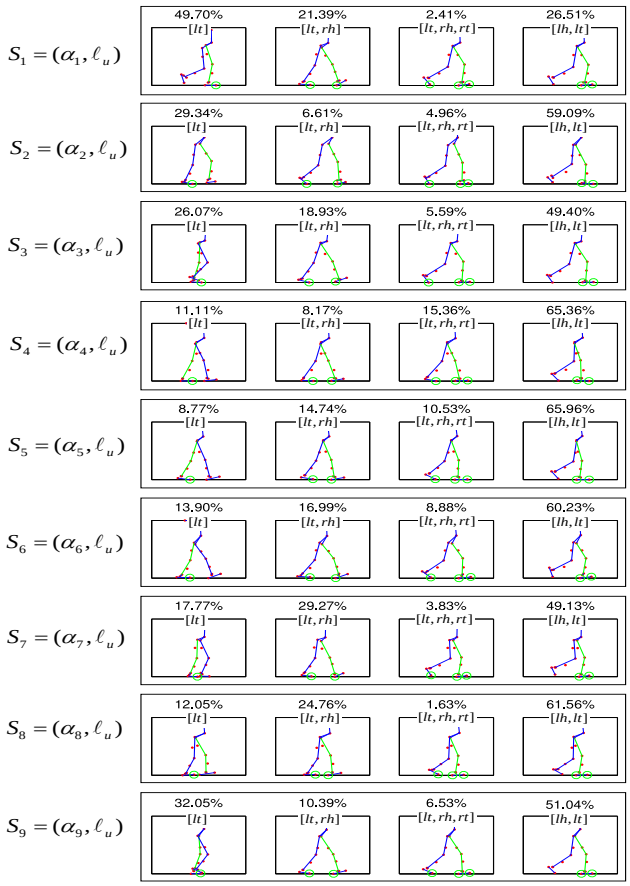

Figure 6: The domain breakdowns without knee lock for the 9 subjects in the order listed in Tab. 3 participating in the experiment, along with the corresponding walking cycle. Each illustration is a snapshot of the subject's configuration at the beginning of the domain. The green circles indicate the contact point that is enforced in a particular configuration.

Subject 1 has a history of back problems (herniated disks at L4-L5 and a pinched nerve at L5-S1) and was taking pain medication at the time of the experiment. Thus, even at the level of comparing human subjects, the HBC seems to identify less "natural" walking.

Due to the high HBC of Subject 1, this subject can be treated as an outlier in the data set. Therefore, it may be desirable to not include this subject in the calculation of the optimal walking cycle. For example, if the HBC were to be used for the detection of medical conditions, one could compile a HBC from healthy subjects. A subject with a suspected medical condition could then be compared to this HBC (much as existing robotic models are compared via the HBC below). To illustrate this idea, we compute the optimal walking cycle from the healthy subjects, or subjects 2-9. This results in the optimal walking cycle:

$$\alpha_2^*(\ell_u) \;:\; 60\% \;\rightarrow\; 17\% \;\rightarrow\; 17\% \;\rightarrow\; 6\%,$$

which has slightly different weightings than α^* due to the exclusion of Subject 1. The corresponding healthy HBC of Subject 1 is computed using α_2^* resulting in a slightly

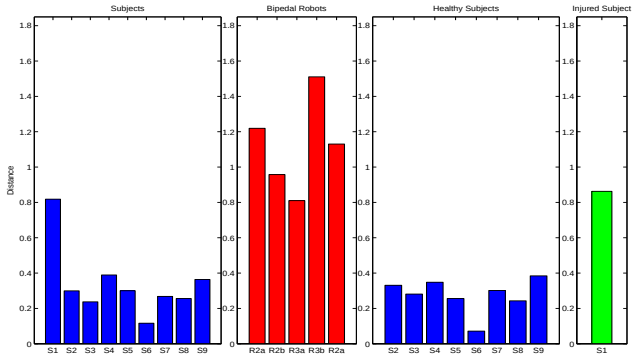

Figure 7: The HBC for the 9 subjects in the experiment and 5 bipedal robotic models that have appeared in the literature (the number of domains in each of the models is illustrated via a subscript) using α^*, and the HBC for the 8 healthy subjects and the "injured" subject using α_2^*.

higher cost than the HBC associated with α^* as expected (0.8628 as opposed to 0.8183). The healthy HBC for all of the subjects using α_2^* is illustrated in Fig. 7. Note that due to the exclusion of the "injured" subject, the costs among the healthy subjects are even more uniform.

Robots. We next use the HBC to compute the cost of walking for bipedal robots that have been considered in the literature with no knee-lock.

In [19], numerous bipedal modes with different numbers of domains (between 1 and 3) and walking gaits are considered. We focus on two with cycles: $\ell_2 : [lh, lt] \rightarrow [lt]$ and $\ell_3^a : [lh, lt] \rightarrow [lt] \rightarrow [lt, rh, rt]$. Associated with the walking found in that paper, there are three walking cycles: $R_{2a} = (\alpha_{2a}, \ell_2)$, $R_{2b} = (\alpha_{2b}, \ell_2)$ and $R_{3a} = (\alpha_{3a}, \ell_3^a)$, for which the HBC can be computed as shown in Fig. 7. From the results of the computed HBC, we conclude that the model R_{3a} produces the most anthropomorphic walking as it has a dramatically lower cost than the other two models. Interestingly, the authors of the paper state that this walking cycle appeared "the closest to human gait" just as the HBC discerns.

In [16], two bipedal walking gaits are obtained with a model consisting of a cycle: $\ell_3^b : [lh, lt] \rightarrow [lt] \rightarrow [rh]$, where $[rh]$ is a domain unseen in the human walking wherein the biped only has a single contact point at the right heel. Associated with this cycle are two walking cycles: $R_{3b} = (\alpha_{3b}, \ell_3^b)$ and $R_{3c} = (\alpha_{3c}, \ell_3^b)$ for which the HBC can be computed; the results are shown in Fig. 7. Interestingly, despite the fact that both of these models have three domains, they do not produce an HBC as low as walking cycle R_{2b} indicating that adding more domains does not necessarily result in more human-like walking.

4.2 HBC with Knee-Lock

For the 9 subjects that performed the walking experiment with associated walking cycles $S_i = (\alpha_i, \ell_i)$ illustrated in Fig. 8, we minimize Equation (6) to find the optimal walking cycle. In performing this minimization we find four optimal walking cycles: $L_i = (\alpha_i^*, \ell_i^*)$, $i = 1, 2, 3, 4$, i.e., four minima with essentially the same cost (3.69, 3.76, 3.79 and 3.94, respectively, with the cost of any other cycle being almost

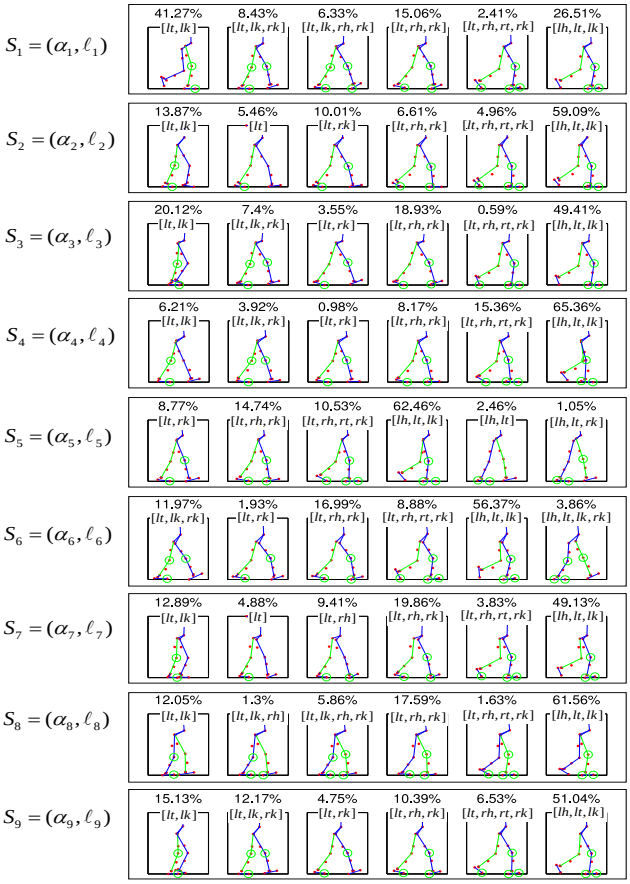

Figure 8: The domain breakdowns with knee lock for the 9 subjects in the order listed in Tab. 3 participating in the experiment, along with the corresponding walking cycle. In this case, there are 13 vertices traversed by the 9 subjects.

twice as high). These optimal walking cycles are shown in Fig. 9.

To determine if one of these optimal walking cycles is preferable to the rest, we can take each of these optimal walking cycles and compute the HBC of the other optimal walking cycles with respect to it as illustrated in the right plot in Fig. 10. Notice that all of the HBCs are nearly uniform. We claim that the "universal" domain graph for bipedal walking with knees is illustrated in Fig. 9 in that any cycle taken in this graph is optimal. The interesting aspect of this domain graph is that, as pointed out earlier, walking with knee-lock is more suited to robots than humans. As such, the domain graph chosen is a design decision in the modeling of the robot so the specific cycle chosen in the "universal" domain graph can be guided by the robot being designed.

Humans. The human-based cost associated with each of the optimal walking cycles computed for each subject in the experiment is illustrated in Fig. 10. One can see that each optimal gives a very similar HBC, which is both consistent with the fact that they are all optimal and points to the fact that we do, in fact, get a "single" human-based cost for all intents and purposes. Looking at the computed human-based

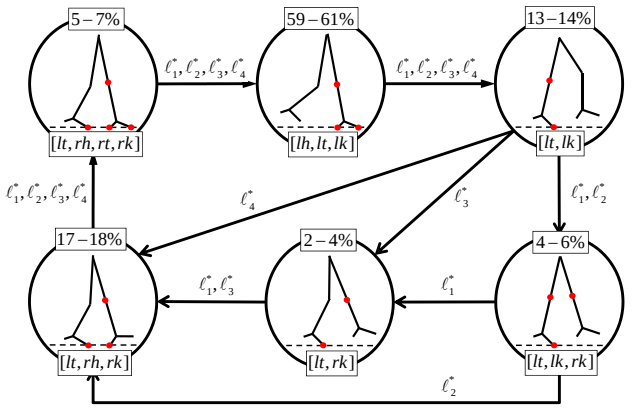

Figure 9: The "universal" domain graph for bipedal walking with knee-lock, consisting of the four optimal walking cycles, with the weight of each cycle on each domain taking values in the indicated interval and the path traversed by the cycle indicated by the edge labels.

costs, Subject 1 again has the largest cost, again consistent with the previously mentioned medical conditions. Interestingly, notice that Subject 8 has the lowest cost. This subject is the oldest, at 77 years of age. Since older individuals tend to walk with a "stiffer" gait, and because knee lock does not appear to naturally occur during human walking, we postulate that the low HBC is identifying this additional stiffness. This observation could have important health care ramifications.

Robots. We also can use the HBC to compare the anthropomorphic nature of different walking gaits for robots with knees-lock that have appeared in the literature consisting of a single domain, R_1 (corresponding to the straight-leg walking of the compass gait biped [9, 12]), two domains, R_2 (corresponding to bipeds with knees that are both unlocked and locked throughout the walking [1, 7, 13]) and both four and five domain models with both knees and feet, R_4 and R_5, respectively [11, 17]. We can compute the HBC for these different robotic walking gaits with respect to the 4 optimal walking gaits as illustrated in Fig. 10. From the computed cost it is clear that as the number of domains increases to better represent the universal domain breakdown in Fig. 9, the HBC decreases accordingly. In particular, R_4 and R_5 have substantially lower HBC than the other robotic walking cycles due to the additional domains, all of which can be found in the "universal" domain breakdown for knee-lock as shown in Fig. 9. In fact, the only domain found in these two walking cycles that is not found in the "universal" domain breakdown is $[lh, lt, lk, rk]$, and the time spent in this domain is small enough, while the time spent in the other domains (which is startlingly similar to the time spent in these domains for the optimal walking cycles) is large enough to deliver a low HBC.

5. CONCLUSION

This paper presented a "universal" domain breakdown and corresponding optimal walking cycle, both without and with knee-lock, obtained from human walking data. From this, the human-based cost was constructed. It was demonstrated

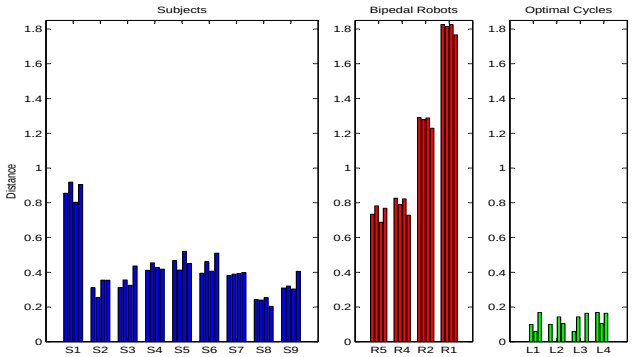

Figure 10: The HBC **for the 9 subjects in the experiment computed with the 4 optimal walking cycles found (left), 4 bipedal robotic models that have appeared in the literature (middle) (the number of domains in each of the models is the subscript), and the** HBC **of each optimal walking cycle computed with the remaining 3 optimal walking cycles (right).**

that when the HBC was computed for the human-subjects preexisting medical conditions were successfully identified. When the HBC was computed for existing bipedal walking robots, the robots with more "human-like" walking gaits were correctly identified. This points to the usefulness of the HBC both in identifying medical conditions in humans, and obtaining anthropomorphic walking in bipedal robots. The results of this paper are also applicable to future bipedal robot design. If the universal domain breakdown is used for the robotic model, and the parameters of the controller used to achieve walking are chosen so as to minimize the HBC, we claim that the end result promises to be natural and human-like walking.

6. REFERENCES

[1] A. D. Ames, R. W. Sinnet, and E. D. B. Wendel. Three-dimensional kneed bipedal walking: A hybrid geometric approach. In *Hybrid Systems: Computation and Control*, San Francisco, CA, 2009.

[2] T. Andriacchi and E. Alexander. Studies of human locomotion: past, present and future. *Journal of Biomechanics*, 33(10):1217–1224, 2000.

[3] C. Borgs, J. Chayes, L. Lovász, V. Sós, and K. Vesztergombi. Convergent sequences of dense graphs I: Subgraph frequencies, metric properties and testing. *Advances in Mathematics*, 219(6):1801–1851, 2008.

[4] D. J. Braun and M. Goldfarb. A control approach for actuated dynamic walking in bipedal robots. *IEEE Transactions on Robotics*, 25:1–12, 2009.

[5] C. Chevallereau, J. Grizzle, and C. Shih. Asymptotically stable walking of a five-link underactuated 3D bipedal robot. *IEEE Transactions on Robotics*, 25(1):37–50, 2009.

[6] J. H. Choi and J. W. Grizzle. Planar bipedal walking with foot rotation. In *American Control Conference*, 2005.

[7] S. H. Collins, M. Wisse, and A. Ruina. A 3-D passive dynamic walking robot with two legs and knees. *International Journal of Robotics Research*, 20:607–615, 2001.

[8] M. Garcia, A. Chatterjee, and A. Ruina. Speed, efficiency, and stability of small-slope 2D passive dynamic bipedal walking. In *IEEE International Conference on Robotics and Automation*, 1998.

[9] A. Goswami, B. Thuilot, and B. Espiau. Compass-like biped robot part I : Stability and bifurcation of passive gaits. Rapport de recherche de l'INRIA, 1996.

[10] J. Grizzle, G. Abba, and F. Plestan. Asymptotically stable walking for biped robots: Analysis via systems with impulse effects. *IEEE Transactions on Automatic Control*, 46(1):51–64, 2001.

[11] J. W. Grizzle, C. Chevallereau, A. D. Ames, and R. W. Sinnet. 3d bipedal robotic walking: Models, feedback control, and open problems. In *NOLCOS*, Bologna, Italy, 2010.

[12] T. McGeer. Passive dynamic walking. *The International Journal of Robotics Research*, 9(2):62, 1990.

[13] T. McGeer. Passive walking with knees. In *IEEE International Conference on Robotics and Automation*, Cincinnati, OH, 1990.

[14] R. M. Murray, Z. Li, and S. S. Sastry. *A Mathematical Introduction to Robotic Manipulation*. Boca Raton, FL, 1993.

[15] K. Ono, T. Furuichi, and R. Takahashi. Self-excited walking of a biped mechanism with feet. *The International Journal of Robotics Research*, 23(1):55, 2004.

[16] T. Schaub, M. Scheint, M. Sobotka, W. Seiberl, and M. Buss. Effects of compliant ankles on bipedal locomotion. In *IROS*, St. Louis, Missouri, USA, 2009.

[17] R. W. Sinnet and A. D. Ames. 2D bipedal walking with knees and feet: A hybrid control approach. In *48th IEEE Conference on Decision and Control*, Shanghai, P.R. China, 2009.

[18] R. Tedrake, T. Zhang, and H. Seung. Learning to walk in 20 minutes. In *Proceedings of the Fourteenth Yale Workshop on Adaptive and Learning Systems*, New Haven, Connecticut, USA, 2005.

[19] D. Tlalolini, C. Chevallereau, and Y. Aoustin. Comparison of different gaits with rotation of the feet for planar biped. *Robotics and Autonomous Systems*, 57:371–383, 2009.

[20] E. R. Westervelt, J. W. Grizzle, C. Chevallereau, J. Choi, and B. Morris. *Feedback Control of Dynamic Bipedal Robot Locomotion*. Control and Automation. Boca Raton, FL, June 2007.

[21] D. A. Winter. *Biomechanics and Motor Control of Human Movement*. Hoboken, NJ, 2005.

[22] F. Zajac, R. Neptune, and S. Kautz. Biomechanics and muscle coordination of human walking-Part I: Introduction to concepts, power transfer, dynamics and simulations. *Gait and Posture*, 16(3):215–232, 2002.

[23] V. Zatsiorky, S. Werner, and M. Kaimin. Basic kinematics of walking: step length and step frequency: a review. *Journal of sports medicine and physical fitness*, 34(2):109–134, 1994.